LA-UR-02-0086

# CASE STUDIES–INTERNAL DOSIMETRY CALCULATIONS USING MARKOV CHAIN MONTE CARLO

Chapter 8 of Practical Applications of Internal Dosimetry
Wesley Bolch, Editor
Medical Physics Publishing 2002

by

Guthrie Miller
Los Alamos National Laboratory
Los Alamos, NM 87545, U. S. A.

January 10, 2002

## 8.1 Introduction

Internal dosimetry may be divided into two main problems: 1) the forward (scientific) problem of determining biokinetic models that describe how radionuclides are taken into the body, distributed in body tissues, and excreted, and 2) the inverse (mathematical) problem: given agreed-upon biokinetic models and the measured amounts in excreta, to determine the times and amounts of intakes into the body.

The forward problem has received a large amount of attention (including the other chapters of this book) and standard biokinetic models are now available for most nuclides (e.g., ICRP publications 30, 54, 66, and 78). The inverse problem has received little attention within the health physics community. The inverse problem requires forward model calculations. An important step forward in this area is the IMBA suite of programs described in the next chapter.(Birchall et al. 1998) These programs will provide working internal dosimetrists with a user friendly means of performing forward calculations (as well as fitting bioassay data) and, in phase II, convenient access to the Bayesian method for the inverse problem described here.

A typical problem confronting an internal dosimetrist is the interpretation of routine bioassay monitoring data where times of possible intakes are not known. Often individual cases are laboriously treated on a case-by-case basis, using "professional judgment" to decide when and if multiple intakes may have occurred. Or, automated methods are used that assume each new measurement is associated with a new intake occurring midway in time between the new measurement and the last measurement. These types of data unfolding procedures(Lawrence 1962)(Ward & Eckerman 1992) often overfit the data resulting in intake scenarios that are strongly fluctuating, including negative values. Also, there is not always proper statistical weighting of data; all data points are sometimes treated equally regardless of their uncertainty estimates. A Bayesian unfolding scheme(Miller et al. 1999) remedies some of these problems but does not properly treat the determination of multiple intakes.

The inverse problem of internal dosimetry is, in fact, a generic problem widely studied in other fields (for example in image reconstruction, spectral deconvolution, and model parameter fitting). Miller and Inkret have described a code for plutonium internal dosimetry (Miller & Inkret 1996) using the maximum entropy method (Skilling 1989), a widely used method for underdetermined inverse problems with a positivity constraint. The new code offers some substantial advantages: it ensures positive intakes and doses, it smooths out fluctuating data, and it provides an estimate of the propagated uncertainty in the calculated intakes or doses. However, 1) because the code does not allow the use of a realistic prior (the prior must be the entropy function) and 2) the code does not calculate posterior probability distributions (only finding the maximums of the posterior probability), we do not believe it to be satisfactory.

One of the main disadvantages of Bayesian approach has been the lack of guidance in the choice of the prior probability distribution, which is always necessary in the Bayesian statistics. The Bayesian health physicist is allowed to choose the prior probability distribution subjectively. We prefer, however, to determine the prior from relevant data whenever possible. The prior probability distribution has a small effect on the inferred result when a large amount of measurement data are available. In the opposite case, which is not unknown in health physics, the prior can influence the inference in an important way.

In (Miller et al. 2001) some theoretical concepts and historical data from tritium and plutonium internal dosimetry at Los Alamos were used to arrive at suitable, simple models for the prior probability distribution. Two models for the prior probability distribution were proposed: 1) the log-normal distribution, when there is some additional information to determine the scale of the true result, and 2) the "alpha" distribution (a simplified variant of the gamma distribution) when there is not.

At the practical level for internal dosimetry, these new models for the prior probability distribution have been incorporated into our Bayesian internal dosimetry codes. In order to carry out a Bayesian analysis of bioassay data using the new models for the prior probability distribution, the internal dosimetrist need only choose the value of a single parameter. When the worker has been involved in an incident or incidents, the prior parameter characterizes the additional information on the possible magnitude of the intake (for example, nose swabs or air monitor readings). When no incidents have occurred, the prior parameter reflects the population average of the number of intakes (in a certain range of magnitude) that occur per unit time. From Los Alamos plutonium data in recent years, this number (the parameter $\alpha$) is about 1 "intake" per 1000 workers per year or even less.

The inverse problem of internal dosimetry is to use the bioassay measurements and a set of agreed-upon biokinetic models to infer if and when intakes may have occurred and the magnitude of the resultant radiation dose to the worker. This problem is naturally posed as a problem of Bayesian inference. The Markov Chain Monte Carlo (MCMC) method (Miller et al. 2002a, Gilks et al. 1996) provides an exact solution of the Bayesian inference problem without simplifying assumptions. In this chapter three plutonium internal dosimetry cases are analyzed using the MCMC code ID1.1 and described in some detail.

Many health physics measurements involve counting, usually in conjunction with a background count, which is subtracted in some way. The likelihood function in these cases involves Poisson distributions (for long decay times). Optional use of exact likelihood functions in our Bayesian internal dosimetry codes has been implemented using an interpolation-table approach.(Miller et al. 2002b) This means that the exact likelihood functions can be used with no computation time penalty except for the initial setup of the interpolation tables.

In cases with only a few measurements involving low-level counts, we find that sometimes significant errors are made using the Gaussian approximation rather than the exact likelihood function. One such case will be discussed in this chapter.

An introductory discussion of the use of Bayesian methods for internal dosimetry is contained in a recent review paper (Miller et al. 2000).

## 8.2 Statistical Inference

The forward problem of mathematical modeling consists of calculating quantities of interest from a model that is thought to represent the physical system of interest, given values of the set of parameters of the model. Biokinetic models are examples of such models. Present biokinetic models are quite simple in one sense, in that they are linear, so that they may be summarized for all intake values by interpolation tables. The actual calculation of present biokinetic models is somewhat complex, involving the simultaneous solution of a fairly large number of ordinary linear differential equations. This system of equations usually, but not always, has constant coefficients, allowing the use of linear algebra solution techniques.

The inference problem is to determine "best" values of the parameters from the measurement data, using agreed-upon forward models. This type of generic problem is extremely common and there are several well known techniques, for example $\chi^2$ minimization or maximum likelihood. In recent years the Bayesian method has begun to replace these older methods, because of its more appealing conceptual basis and because the computational power needed is now becoming readily available.

The Bayesian method is quite simple and elegant to formulate. Letting $X$ denote the data (a multidimensional vector quantity), and $\xi$ denote the parameters (another vector quantity, usually with higher dimensionality than the data), the inference problem is to determine $P(\xi|X)$, read as the probability of parameters $\xi$ given the measurements $X$ (for continuous variables, $P(.|X)$ is a probability distribution function rather than a discrete probability). Rather than seeking to determine a single "best" value of the parameters, we recognize from the outset that there are considerable uncertainties involved and the probability distribution of the parameters is the quantity of interest. The probability distribution of the parameter values given the measurements may be such that it can be summarized by a central value (average, median) and a width estimate (standard deviation, credible limits), or it may be too complex to simply characterize (long tail, bimodal). The crucial conceptional step is to accept that the inferred parameters are random variables.

The rest follows from logic and mathematics and is the famous and controversial Bayes theorem:

$$P(\xi|X) \propto P(X|\xi)P(\xi). \tag{1}$$

The proportionality means that a normalization factor independent of $\xi$ is needed.

In Eq. 1 $P(X|\xi)$ is the probability of measurements $X$ given the parameters $\xi$. This is the probability distribution that is usually studied and thought about in connection with a measurement. For example, the parameter might be the (unknown) true mean number $\mu$ of counts in a counting measurement system and the data the actual number $N$ of counts observed, which follows the Poisson distribution

$$P(N|\mu) = \frac{\mu^{N} e^{-\mu}}{N!}.$$

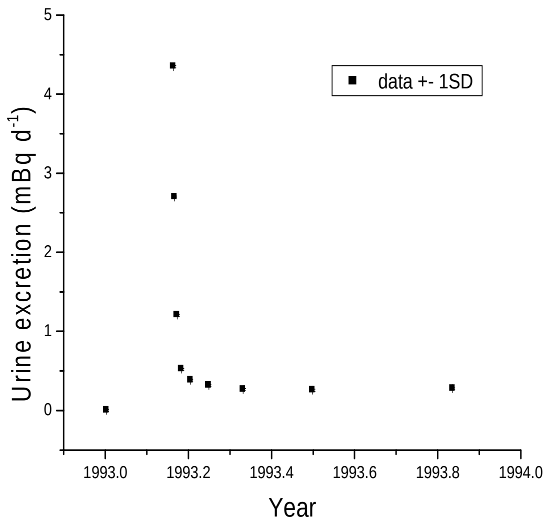


Figure 1: Test $^{239}$Pu urine data.

Considered as a function of $\xi$, $P(X|\xi)$ is called the likelihood function. That it appears in Eq. 1 seems quite reasonable. The other quantity on the right hand side of Eq. 1 is more contentious. It is called the prior probability distribution. We prefer to think of the prior in entirely objective terms as the probability distribution of $\xi$ in the measured population. This is illustrated later on in this chapter for an example involving background counting rates.

Equation 1 is the solution of the inference problem. All that is needed is to integrate over subsidiary variables to display the probability distribution of the quantities of interest. For example, consider an internal dosimetry problem with 40 possible intakes where there are 120 parameters (the time, amount, and type of each intake). We may wish to examine the distribution of total CEDE for all intakes summed together, so it is necessary to integrate out (marginalize) the detailed probability distribution function given by Eq. 1 with respect to the other variables. This integration is performed using the MCMC method.

## 8.3 Case I-Code validation

This case involves simulated $^{239}$Pu urine excretion data, calculated using an assumed intake amount (370 Bq), a biokinetic type (ICRP-30 class Y, 1 $\mu$m AMAD), and date of intake (28- February-1993). These data are shown in Fig. 1. The data are assumed to have rather small measurement uncertainties (the 1 SD uncertainty error bars are too small to be visible in Fig. 1), roughly corresponding to the measurement uncertainty obtained using Thermal Ionization Mass Spectrometry (TIMS (Inkret et al. 1998)). A multiplicative uncertainty SD of 0.3 is also assumed. This would correspond to the biological/sample collection uncertainty for simulated 24-hr urine samples normalized using sample volume and specific gravity. The code assumes an intake in each of the intervals between bioassay data points (9 intakes). The multivariate posterior distribution of amount, time, and biokinetic type for each intake given by Bayes theorem is integrated using the MCMC technique.(Miller et al. 2002a)

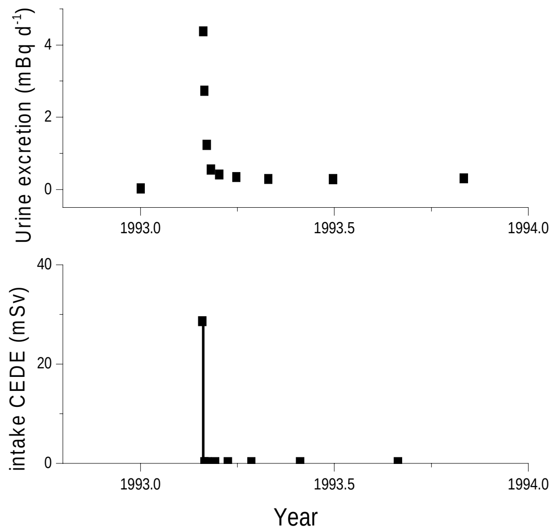


Figure 2: Test $^{239}$Pu urine data and calculated (posterior average) intake amounts.

In Fig. 2 are shown the bioassay data together with the average value of the calculated intakes (in terms of CEDE) and intake times. There is only one significant calculated intake. The posterior distribution of intake dates for the significant intake is shown in Fig. 3, where fractional time corresponds to the 2-month interval between the first and second bioassay data points. The date distribution correctly peaks at 28-February-1993.

The posterior distribution of biokinetic types is shown in Fig. 4. The "universe" of possible biokinetic types is shown in Fig. 4, using the following labeling scheme. The first character "I" stands for inhalation. The second character is either 1) "Y", for ICRP-30 class Y, or 2) "W" for class W. The third character denotes one of three particle sizes, 1) "S" for small (0.2 $\mu$m AMAD), 2) "M" for medium (1 $\mu$m AMAD), and 3) "L" for large (5 $\mu$m AMAD). As seen, by far the most probable biokinetic type is IYM, inhalation of class Y medium particle size, which is the correct result.

Figure 5 shows the calculated distribution of intake amount in terms of CEDE. The correct result is 28.7 mSv, very close to the median value of the cumulative probability distribution. There are two curves overplotted in Fig. 5: 1) the initial parameter values of the Markov Chain chosen to be the minimum possible values, and 2) the initial parameter values chosen to be the maximum possible values with a different value of the random number seed. The fact that the two curves agree is taken as an empirical measure of convergence, that is, that an adequate number of chain iterations have been calculated.

The Bayesian formalism allows us to consider any function of the parameters. Any such function will have a posterior statistical distribution. A natural quantity of interest is the calculated urine excretion at the times of the bioassay measurements. Fig. 6 shows measured data together with the average (or expectation) value of the calculated excretion.

One of the primary features of the Bayesian method is that it allows the calculation of the probability distribution of quantities of interest, given the measurements. Such a posterior distribution of CEDE of the first intake was shown in Fig. 5. Other methods of displaying this information may be helpful. Figure 7 shows the average value of CEDE for all the

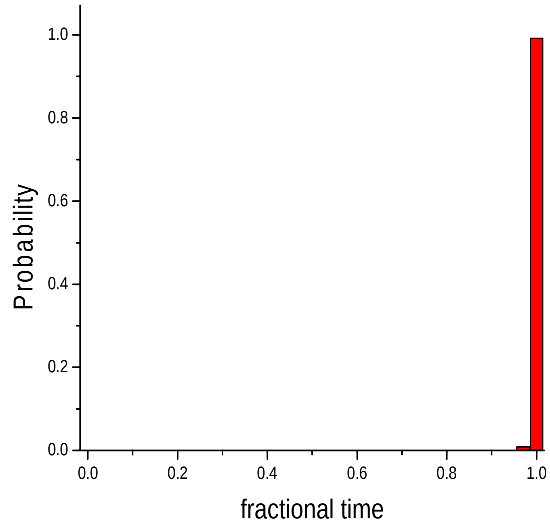


Figure 3: Posterior distribution of time of intake for the large calculated intake using $^{239}Pu$ test urine data.

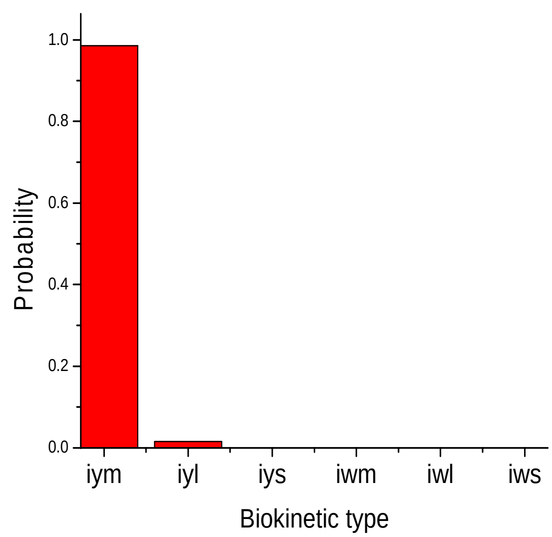


Figure 4: Posterior distribution of biokinetic type for the large calculated intake using $^{239}Pu$ test urine data.

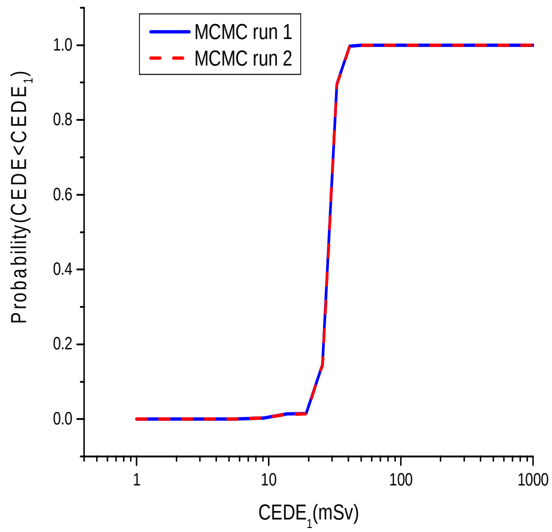


Figure 5: Cumulative posterior distribution of intake amount for the large calculated intake using $^{239}Pu$ test urine data.

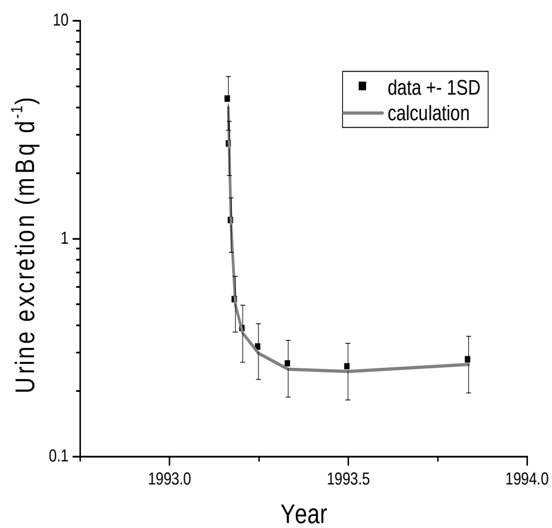


Figure 6: Average of the posterior distribution of calculated urine excretion for the large calculated intake using $^{239}Pu$ test urine data.

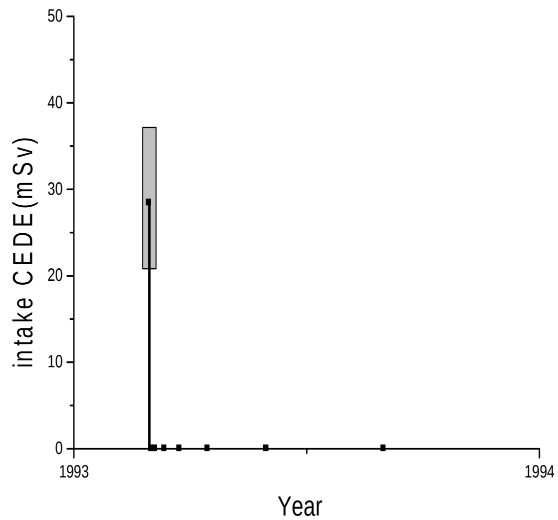


Figure 7: Average values and 5% and 95% credible limits of calculated CEDE for all intakes using $^{239}$Pu test urine data.

intakes along with shaded bars representing the 5% and 95% credible limits for those cases where the upper credible limit exceeds 1 mSv. There may be cases where the average value exceeds the upper credible limit (when the distribution is narrowly peaked at 0, but with a long tail). Figure 8 shows a shaded contour plot of the posterior distribution of CEDE for intake 1. This type of representation may be more intuitive than others that require an understanding of X-Y plots.

The accurate and precise data assumed for this test case allows the calculation to correctly select the biokinetic type. Thus if we run the calculation assuming only one biokinetic type, "IYM" (the correct one), we obtain in Fig. 9 essentially the same result as shown in Fig. 5.

This is not usually the case as will be discussed later on. By using the very same calculated data (central values) with larger assumed uncertainties we can illustrate the importance of measurement precision in obtaining accurate internal dose assessments. The assumed measurement uncertainty is now increased by an order of magnitude (roughly corresponding to the measurement uncertainty of Radiochemical Alpha Spectrometry-RAS). These data are shown in Fig. 10. In the case of larger measurement uncertainty, the correct biokinetic type is no longer singled out by the data as shown in Fig. 11. The data over the 8-month collection time span are not precise enough to distinguish class Y from class W behavior. As a consequence the posterior distribution of CEDE from the first intake now extends down to the smaller doses obtained if class W is assumed as shown in Fig. 12.

In Fig. 12 one can see a typical example of incomplete convergence. Our interpretation of such a plot is that the correct result is probably somewhere between the two cases shown. To remedy the convergence problem the code would be run for a larger number of iterations, if this is feasible.

Figure 13 shows that the breadth of the posterior distribution of CEDE is indeed caused by the uncertainty of biokinetic type. If only one biokinetic type is allowed, the distribution is again very narrow, just as in the case of small measurement uncertainties.

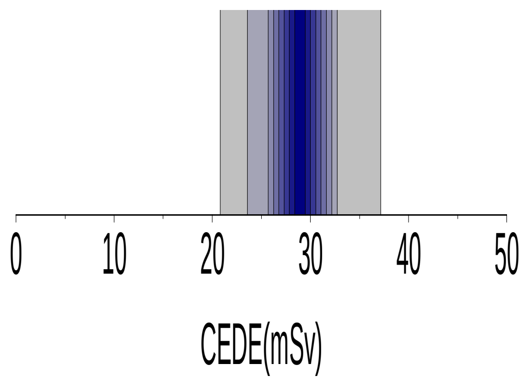


Figure 8: Shaded contour plot of the posterior distribution of CEDE for the large intake calculated using $^{239}Pu$ test urine data.

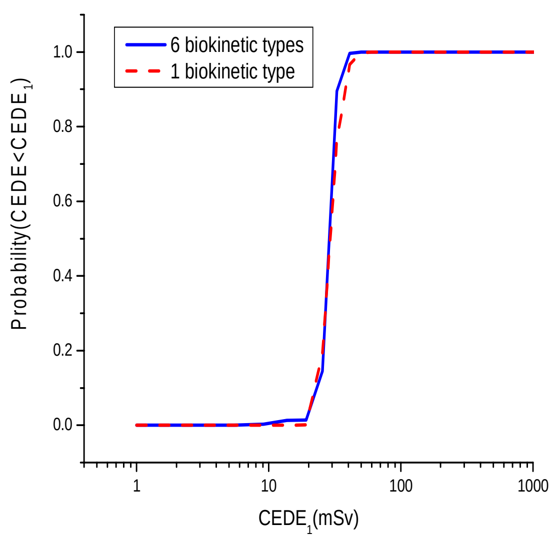


Figure 9: Cumulative posterior distribution of intake amount of the first intake using $^{239}Pu$ test urine data, calculated assuming 6 possible biokinetic types and only 1 biokinetic type.

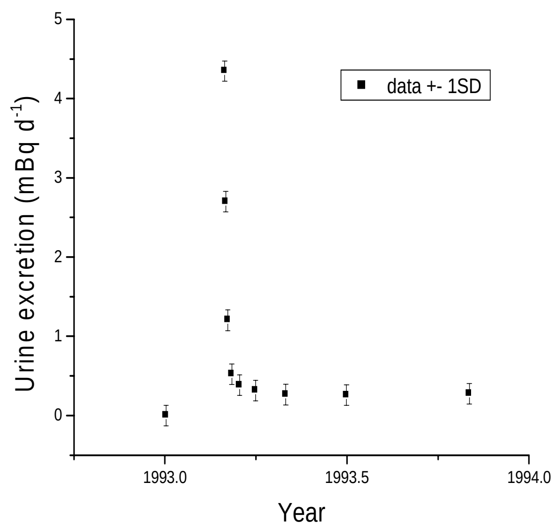


Figure 10: Test $^{239}Pu$ urine data with larger assumed measurement uncertainties.

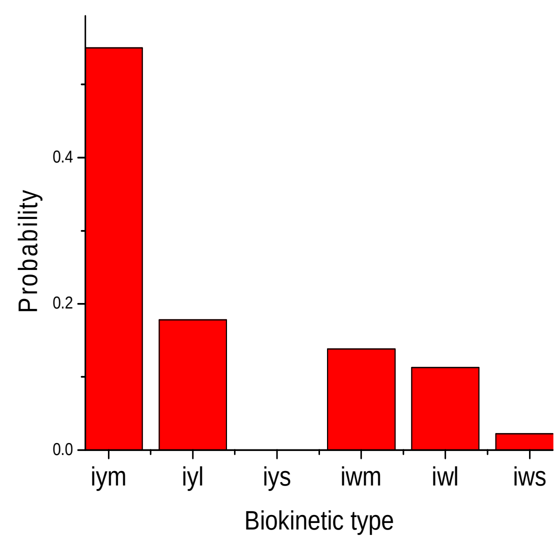


Figure 11: Posterior distribution of biokinetic type calculated using test $^{239}Pu$ urine data with larger assumed measurement uncertainties.

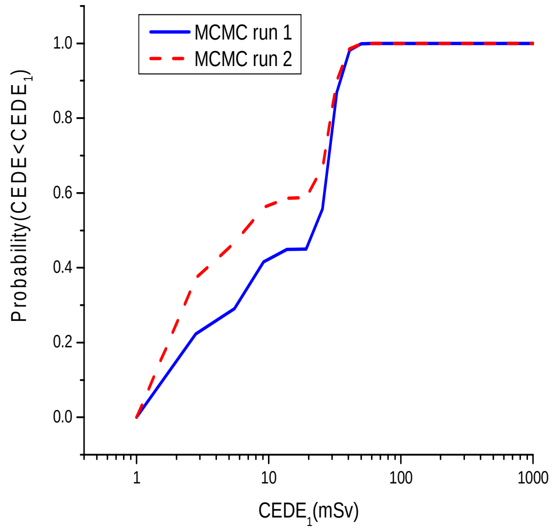


Figure 12: Cumulative posterior distribution of intake amount for the first intake calculated using $^{239}$Pu test urine data with larger assumed measurement uncertainties.

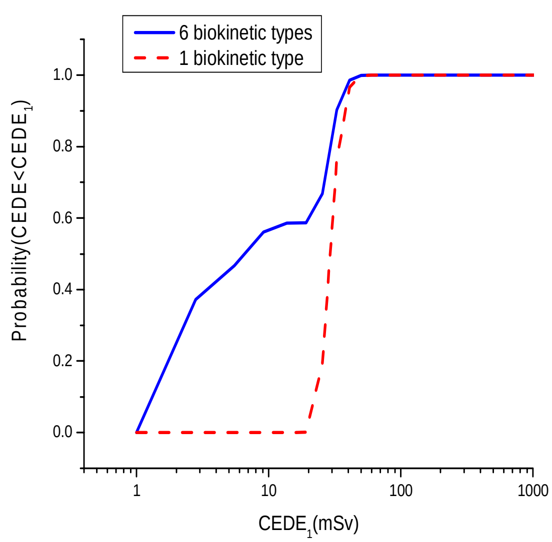


Figure 13: Cumulative posterior distribution of intake amount of the first intake using $^{239}$Pu test urine data with larger assumed measurement uncertainties, calculated assuming 6 possible biokinetic types and only 1 biokinetic type.

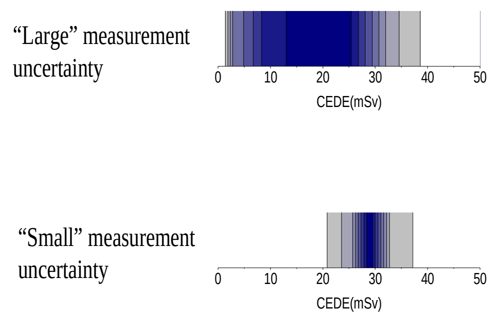


Figure 14: Comparison of shaded contour plots of the posterior distribution of CEDE for the large and small uncertainty cases using $^{239}$Pu test urine data.

Finally in Fig. 14 we compare the uncertainty of the calculated CEDE in the two cases of "small" and "large" measurement uncertainty. Even though the simulated data in both of these cases is very high quality by the usual standards of internal dosimetry, the uncertainty of the calculated CEDE is quite significant in both cases.

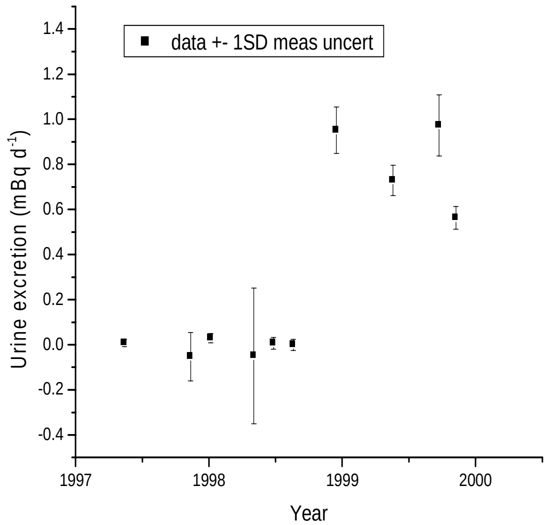


Figure 15: $^{239}$Pu urine data for an actual Los Alamos case.

## 8.4 Case II-overexposure detected from routine urine monitoring

This case involves actual $^{239}$Pu urine excretion data from Los Alamos. This event was termed an overexposure since the calculated CEDE was greater than 50 mSv. A worker had an intake of $^{239}$Pu not associated with workplace indications of a release (for example, elevated air monitor readings, external contamination). This type of non-incident-related intake is extremely rare, and the Bayesian method is very important in such situations to avoid an inordinate number of false positives. The prior probability distribution used to interpret non-incident bioassay plutonium data at Los Alamos is based on studies of a large number of such cases, which shows that the probability of a true intake is less than 1 in 1000 per year.(Miller et al. 2001)

The dataset is particularly interesting in that TIMS measurements were taken along with RAS measurements. A question of interest is whether this intake would have been detected using just the first elevated RAS data point, and how the calculated posterior probability from the first RAS data point compares with result after 4 TIMS measurements. Note that a single TIMS measurement that is 10 times more sensitive than a single RAS measurement is equivalent to 100 RAS measurements. Since TIMS sensitivity exceeds RAS by more than an order of magnitude, the urine excretion pattern should be considered very well characterized with the TIMS data.

Figure 15 shows the urine excretion data. Some of the data points are RAS measurements and others represent the properly weighted average of an RAS measurement and a TIMS measurement.

In Fig. 16 are shown the calculated intakes corresponding to this data. There is only one significant intake. The lower plot shows the average time of each intake and the average amount in terms of CEDE.

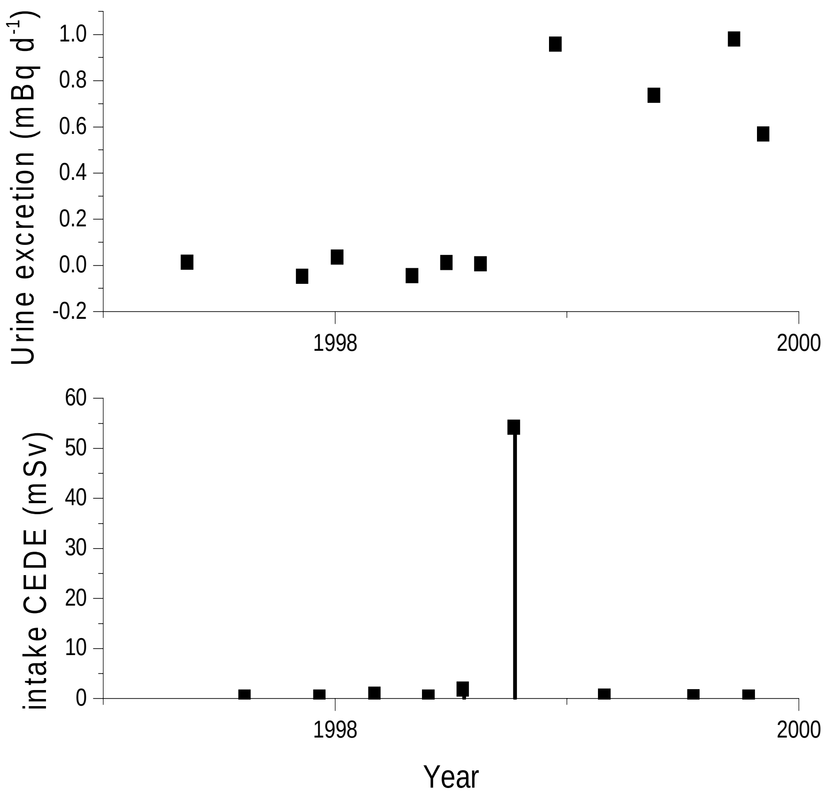


Figure 16: $^{239}$Pu urine data and calculated (posterior average) intake amounts.

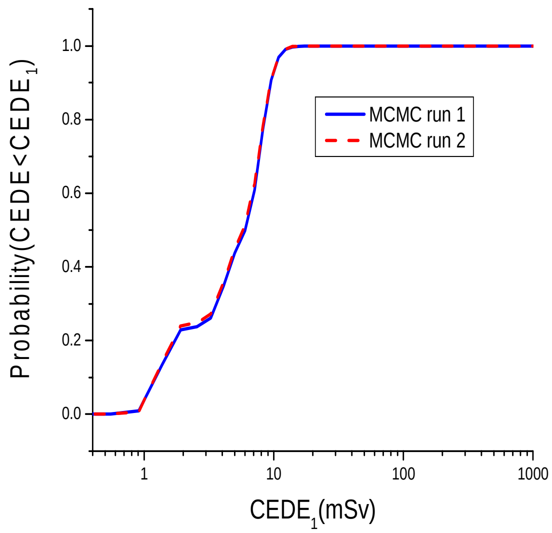


Figure 17: Cumulative posterior distribution of CEDE associated with the large intake calculated from $^{239}$Pu urine data.

Figure 17 is a plot of the cumulative posterior probability of the CEDE associated with the single significant intake. Figures 18 and 19 plot the uncertainty of this CEDE in ways that may be easier to understand. In Fig. 19 we have added a reference line corresponding to natural background radiation. This might help the worker understand the magnitude of his or her intake.

Unlike the code validation case I, we do not know the "correct" answer in this case; however, with the TIMS measurements we have a quite accurate result. We now consider what MCMC calculates with just the RAS data, in particular with only the first elevated RAS result. The RAS measurement results are shown in Fig. 20. The RAS count data are shown in Table 1. In Table 1, $\alpha$ and $\beta$ are parameters of the prior probability distribution of

Table 1: RAS count data.

| sample date | gross counts | background counts* | $t_b/t^\dagger$ | $(\alpha-1)t_b/\beta^\ddagger$ | $\beta/t_b$ |
|---|---|---|---|---|---|
| 19-Aug-1998 | 2 | 1 | 6 | 3.64 | 1.92 |
| 15-Dec-1998 | 15 | 2 | 6 | 3.64 | 1.92 |
| 19-May-1999 | 9 | 2 | 6 | 3.64 | 1.92 |
| 22-Sep-1999 | 12 | 2 | 6 | 3.64 | 1.92 |
| 7-Nov-1999 | 3 | 0 | 6 | 3.64 | 1.92 |

* in counting period $t_b$
† ratio of background counting period to gross counting period
‡ most probable number of background counts in count period $t_b$ from prior

background count rate determined using population data.(Miller et al. 2002b) The parameter $(\alpha-1)t_b/\beta$ is the most probable number of background counts in counting period $t_b$ and $\beta/t_b$ is a measure of the width of the prior probability distribution of background count rate, values greater than 1 corresponding to a narrow distribution. These parameters are discussed in detail in (Miller et al. 2002b) and will be discussed later on here.

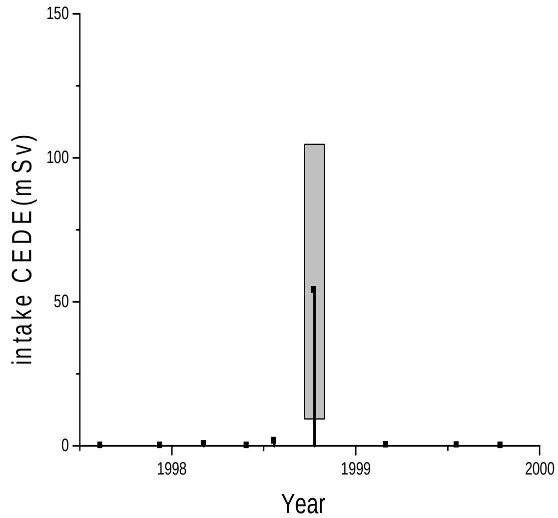


Figure 18: Average values and 5% and 95% credible limits of calculated CEDE for all intakes calculated from $^{239}$Pu urine data.

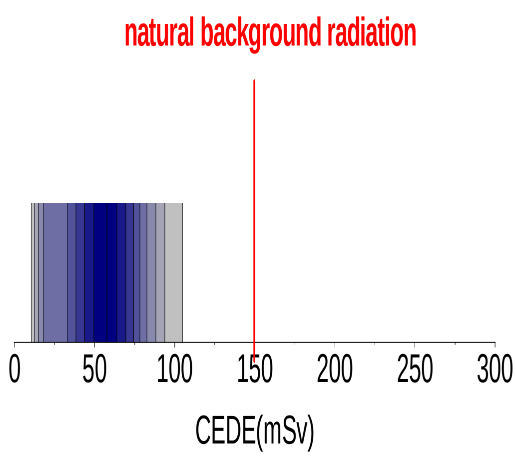


Figure 19: Shaded contour plot of the posterior distribution of CEDE for the large intake calculated for LANL $^{239}$Pu case.

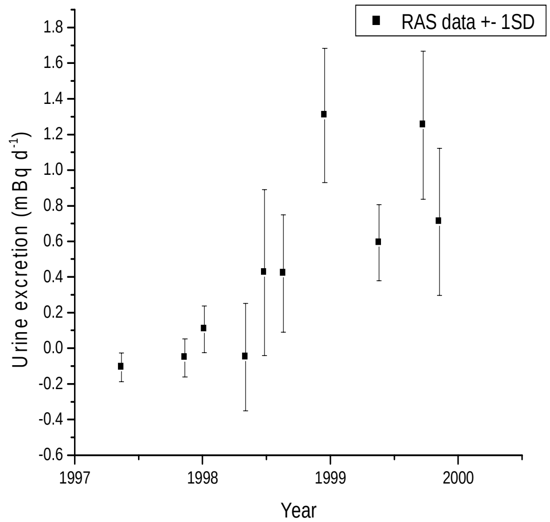


Figure 20: $^{239}$Pu urine data using only RAS count measurements.

Figure 21 shows the posterior probability of CEDE based on the first elevated RAS measurement calculated in two different ways: 1) using the exact Poisson likelihood function, and 2) using the Gaussian approximation.(Miller et al. 2002b) It is clear that the Gaussian approximation leads to a considerably different result than the exact Poisson likelihood.

The exact likelihood calculation involves a Bayesian calculation of the true background count rate. Although not very important numerically, this part of the problem is a nice illustration of the Bayesian method. As in any Bayesian estimation problem, a prior probability distribution is needed. The best way to come up with a prior is to use data. Such data for background count rate are shown in Fig. 22, which shows the distribution of observed background counts for a large number of similar measurements.

The background count distribution is fit by assuming an underlying distribution of true background count rate and using the known Poisson distribution of measured counts, given the true count rate. The fit parameters are the parameters $\alpha$ and $\beta$ of the Gamma distribution shown in Fig. 23. For conservatism, the parameter $\beta$ is not allowed to be too large (larger than $2t_{\mathrm{b}}$) as this implies a very narrow prior distribution. The prior parameters used are shown in Table 1. For example, for the 15-December-1998 measurement there were 15 gross counts and 2 background counts. The 2 background counts are interpreted in light of the fitted Gamma prior distribution of true background count rate, which peaks at 3.64 counts. So the measured 2 counts are effectively pulled up somewhat toward the peak of the prior.

Figure 24 shows the effect of adding a second RAS measurement in narrowing the posterior distribution of CEDE. Figure 24 also adds the “final” result obtained using the TIMS measurements.

In Fig. 25 is shown the progression of knowledge of the true CEDE from the first RAS measurement to the full dataset. The probability distributions are as we would hope them to be. The range of the initial estimate encompasses that of the final estimate.

A dataset limited in time span such as this one cannot hope to distinguish the biokinetic

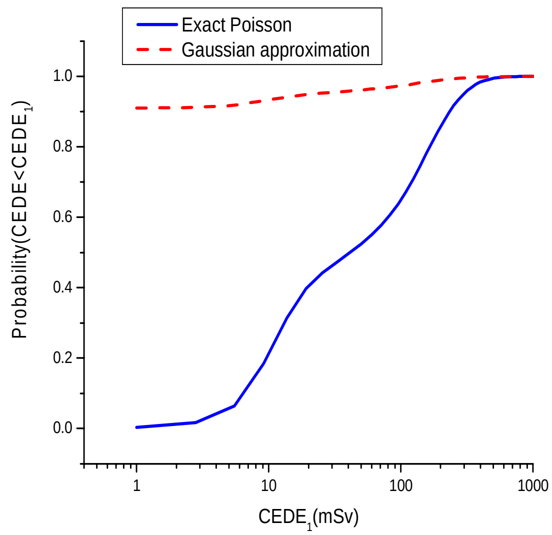


Figure 21: Cumulative posterior distribution of CEDE for LANL $^{239}$Pu case calculated from the first elevated RAS data point using the exact Poisson likelihood and the Gaussian approximation.

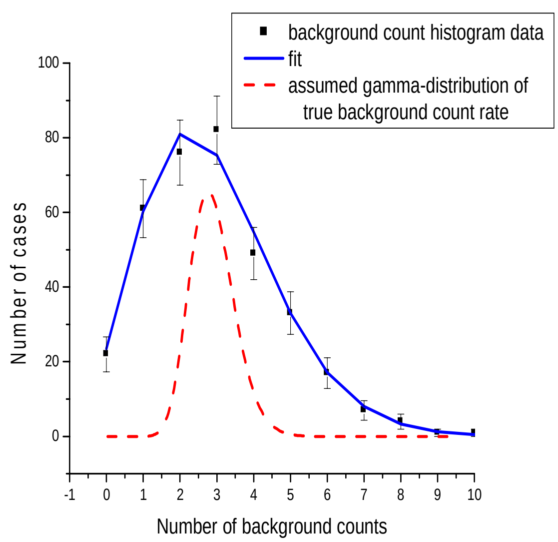


Figure 22: Histogram of the frequency distribution of background counts (in counting period $t_b$) for a large collection of similar cases, together with a fit.

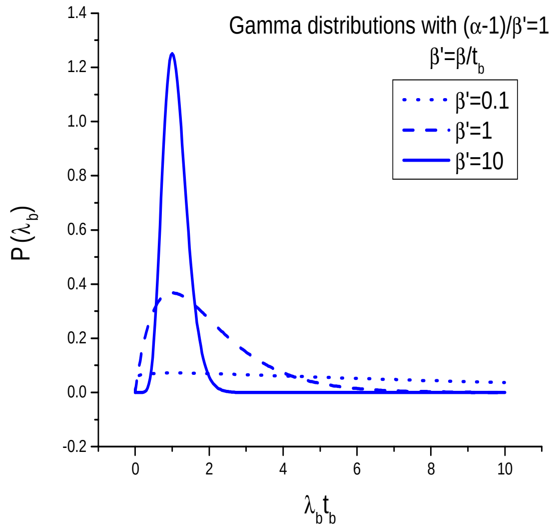


Figure 23: The Gamma distribution for various values of the parameters $\alpha$ and $\beta$.

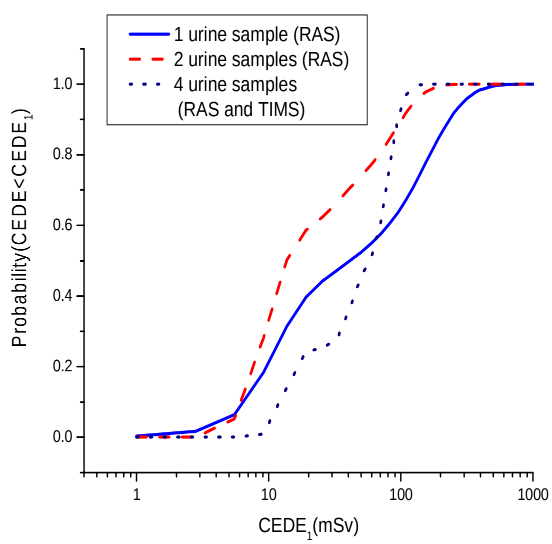


Figure 24: Cumulative posterior distribution of CEDE calculated using 1) the first, 2) the first and second RAS data points, and 3) all data (RAS and TIMS) for LANL $^{239}$Pu case.

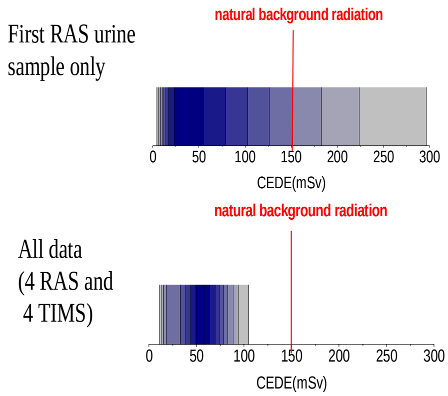


Figure 25: Progression of knowledge of CEDE from first RAS measurement to full data set (4 RAS and TIMS measurements) for LANL $^{239}$Pu case.

type from the excretion pattern. This is shown in Fig. 26, which shows that many biokinetic types are consistent with the excretion pattern of the data.

Also of great practical interest in a case like this is determining the date of intake, in order to try to understand how the release occurred. As Fig. 27 shows, the date of intake is not determined, except that intakes immediately preceding the first elevated urine sample seem less likely.

The Bayesian method works with any agreed-upon set of biokinetic models defining the "universe" of possible biokinetic responses. The effect of using the ICRP-60 family of biokinetic models rather than ICRP-30 models is shown in Fig. 28. As is typical for plutonium internal dosimetry based on urine bioassay, the new models give a CEDE about a factor of 2 less than the old. In this case the CEDE calculated using the ICRP-60 family of biokinetic models no longer exceeds the regulatory limit of 50 mSv. It might be reasonable in some cases to do calculations with a mix of different families of models in order to estimate the uncertainties related to lack of understanding of the biokinetics.

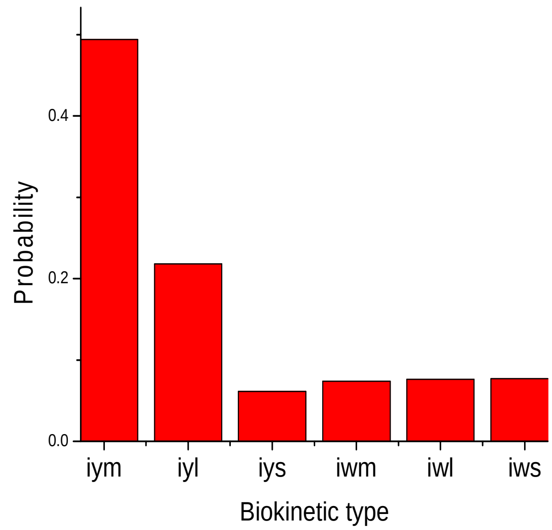


Figure 26: Posterior distribution of biokinetic type for LANL $^{239}$Pu case.

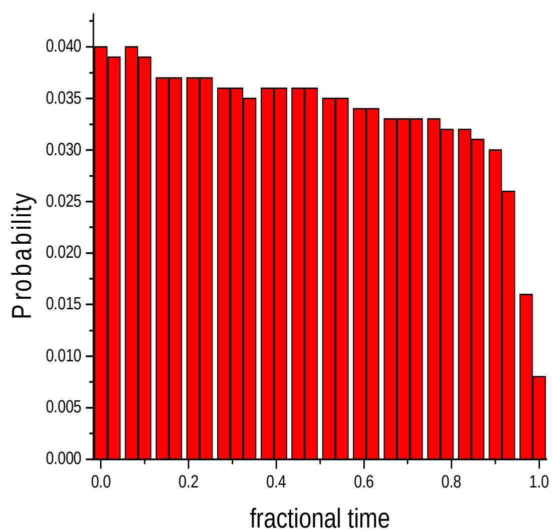


Figure 27: Posterior distribution of intake time (in the time period 19-August-1998 to 15-December-1998) for LANL $^{239}$Pu case.

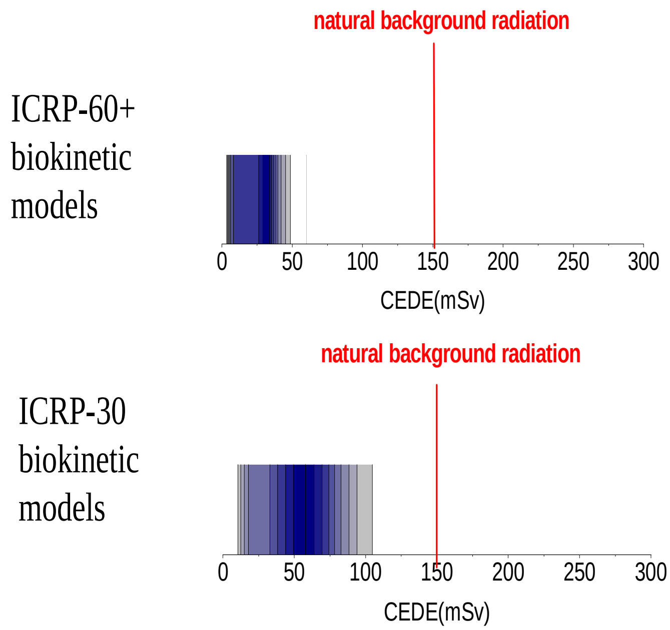


Figure 28: Comparison of CEDE results using ICRP-30 and ICRP-60+ biokinetic models for LANL $^{239}$Pu case.

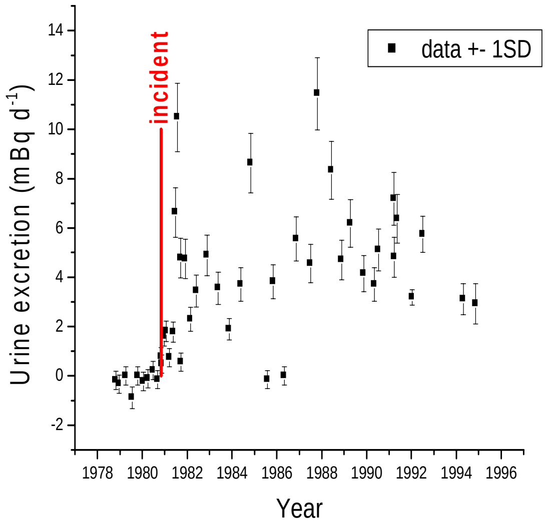


Figure 29: Urine bioassay data for a Los Alamos $^{238}$Pu case.

## 8.5 Case III-Multiple Intakes?

This case involves actual $^{238}$Pu urine bioassay data from Los Alamos. The data are shown in Fig. 29. The dataset is typical of the quality of bioassay data actually encountered in practice. For example, the two low data points occurring around 1986 seem obviously erroneous.

This person was involved in an off-normal event (incident) on 30-October-1980 involving moderate-level workplace indicators (sudden release of $^{238}$Pu when a plastic bag containing contaminated trash ruptured causing an air monitor alarm $\approx$ 60,000 dpm m$^{-3}$, 368/651 dpm nose swipes). Whenever incident information is available, it is incorporated into the prior probability.(Miller et al. 2001) Incidents are categorized into levels of severity and the median value of a broad lognormal prior is chosen accordingly, based on studies of large numbers of similar cases. The MCMC intake scenario calculated for this case, making use of incident information, is shown in Fig. 30. There is only one intake with an appreciable average CEDE, the one associated with the incident. Figure 31 shows the credible limits for each intake in addition to the average value. Two other intakes may have had appreciable CEDEs, but this is uncertain. The average calculated value of the urine excretion is displayed in Fig. 32.

The dominant intake has the distribution of biokinetic types shown in Fig. 33. The most probable biokinetic type is the delayed onset $^{238}$Pu biokinetic behavior identified in the so-called "wing-9" accident that occurred at Los Alamos in 1971.(Hickman et al. 1995, Miller et al. 1999) For $^{238}$Pu, the set of allowed biokinetic types includes this one (denoted IEE for inhalation and the initials of one of the people involved in the 1971 incident) in addition to the standard ICRP-30 types. Delayed-onset biokinetic response is usually misinterpreted using unfolding numerical algorithms (see for example the reconstruction given for this case in (Miller 2000)). In simple cases the fit "by-eye" method might come up with the MCMC-calculated intake scenario, although this is not necessarily likely.

For this case it is interesting to also interpret the data as if the incident information were not available. The MCMC calculated intake scenario, using the standard non-incident prior,

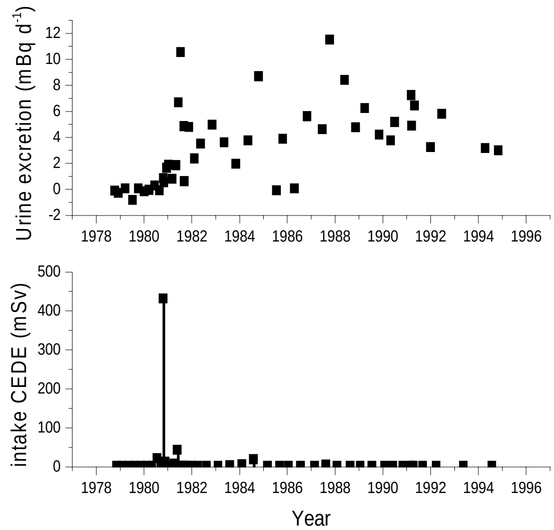


Figure 30: $^{238}Pu$ urine data and calculated (posterior average) intake amounts.

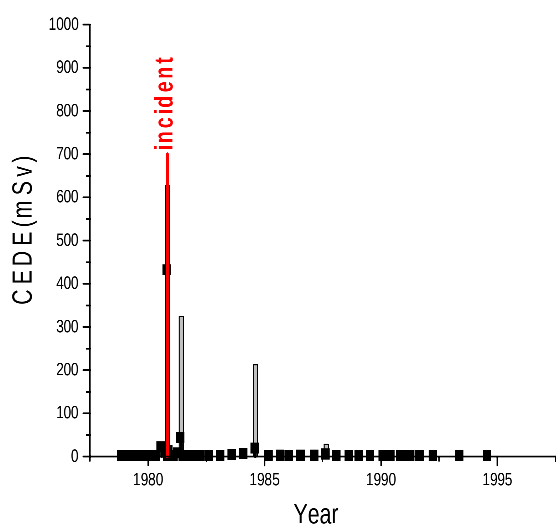


Figure 31: Average values and 5% and 95% credible limits of calculated CEDE for all intakes for LANL $^{238}Pu$ case.

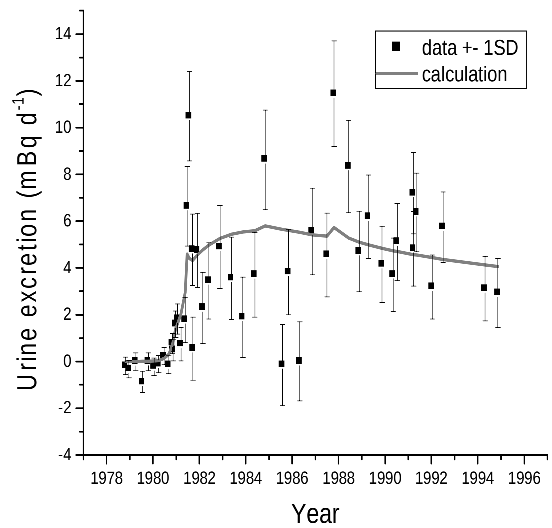


Figure 32: Average of the posterior distribution of calculated urine excretion for the LANL $^{238}$Pu case.

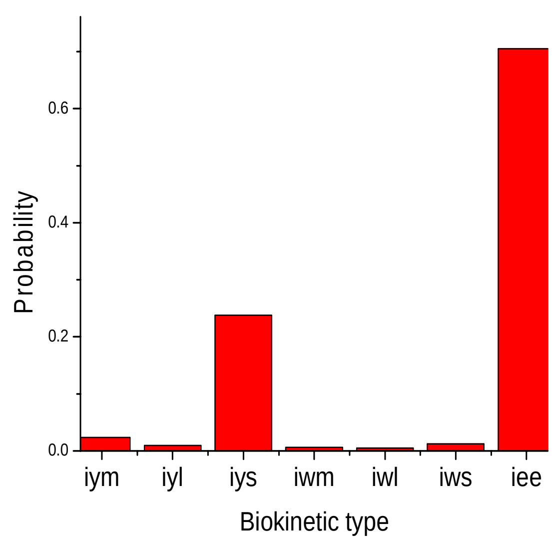


Figure 33: Posterior distribution of biokinetic type for the dominant intake for the LANL $^{238}$Pu case.

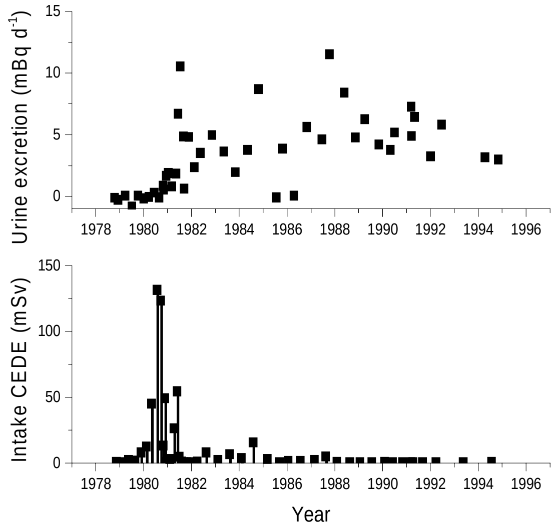


Figure 34: $^{238}$Pu urine data and calculated (posterior average) intake amounts when incident prior is not used.

is shown in Fig. 34. The calculated average CEDE clusters around the time of the incident. Figure 35 shows the calculated intake CEDEs including credible limits.

If instead of a non-incident prior assuming intakes are rare (the intake probability, $\alpha$, is normally taken as 1 in 1000 per year for plutonium work at Los Alamos in recent years(Miller et al. 2001)), we use a non-incident prior with probability of intake 100 times larger (still not including the incident information), the MCMC interpretation is as shown in Fig. 36. This choice of prior probability might be termed a chronic rather than acute intake situation. In Fig. 37 are shown the year-by-year combined intakes (in terms of total CEDE for the year). One would not describe this situation as a single dominant intake, but many intakes. It is not possible to rule out significant intakes over most of the work history. At the same time it is not possible to say with some certainty that an intake occurred except for the yearly combined intake in 1980 and 1981 (when the lower credible limits are greater than 0).

The calculated average urine excretion shown in Fig. 38 better matches the urine data because more intakes (degrees of freedom) are effectively available, because of a prior corresponding to more intakes per unit time.

The computation involved for this case is considerable because of the large number of intakes. The computation time for a single run on a 1 GHz Pentium workstation is given approximately by the formula

$$T = 1.6 \times 10^{-9}\, n_{\mathsf{iter}} N_{\mathsf{in}}^{2.8}, \tag{2}$$

where $T$ is the computation time in minutes, $n_{\mathsf{iter}}$ is the number of chain iterations per intake, and $N_{\mathsf{in}}$ the number of assumed intakes. This case involves 45 intakes and requires about 11 hours of computation time for $10^7$ chain iterations per intake ($45 \times 10^7$ in all). Our rule of thumb is that between 1 and 10 million chain iterations per intake are required for convergence.

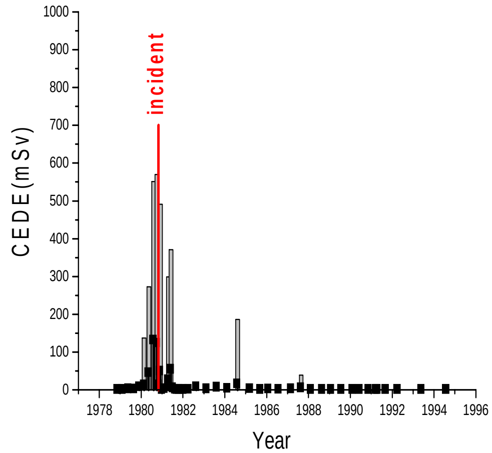


Figure 35: Average values and 5% and 95% credible limits of calculated CEDE for all intakes for LANL $^{238}$Pu case when incident prior is not used.

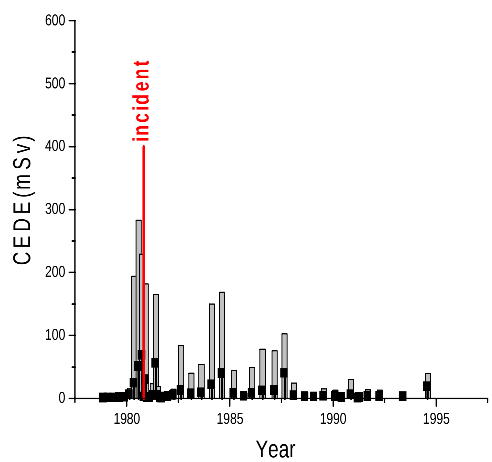


Figure 36: Average values and 5% and 95% credible limits of calculated CEDE for all intakes for LANL $^{238}$Pu case when incident prior is not used and non incident intake probability ($\alpha$) is increased by factor of 100.

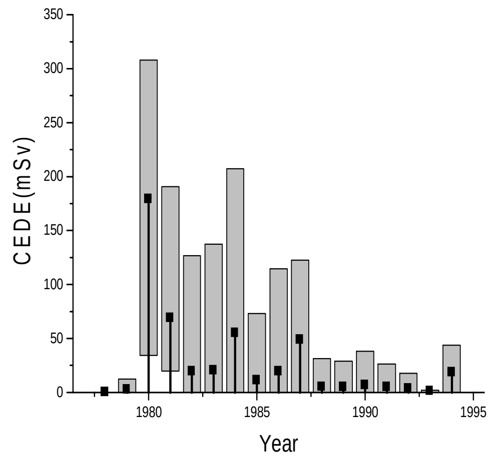


Figure 37: Average values and 5% and 95% credible limits of calculated CEDE for intakes combined on a year-by-year basis for LANL $^{238}$Pu case when incident prior is not used and non incident intake probability ($\alpha$) is increased by factor of 100.

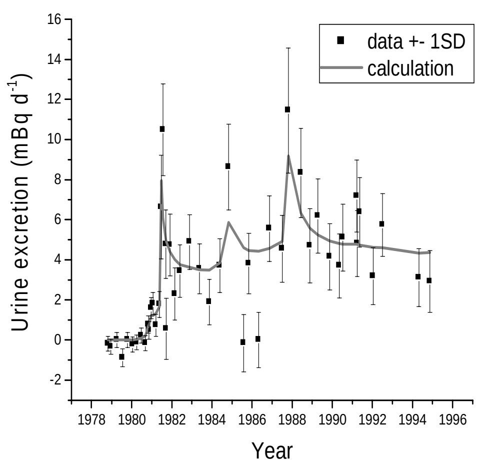


Figure 38: Average of the posterior distribution of calculated urine excretion for the LANL $^{238}$Pu case when incident prior is not used and non incident intake probability ($\alpha$) is increased by factor of 100.

## 8.6 Conclusions

Three plutonium internal dosimetry cases involving urine bioassay have been considered, with a decreasing level of knowledge of the "correct" answer. In the first case, calculated data are used, so complete knowledge of the correct answer is available. The data set consists of nine urine bioassay measurements with equal spacing of the logarithm of time post-intake. If the measurement uncertainty is small enough, the correct date of intake, biokinetic type, and intake amount is faithfully reproduced. Otherwise, primarily because the excretion pattern is not determined precisely enough to single out the correct biokinetic type, the calculated posterior distribution of CEDE is quite broad.

The second case involved actual $^{239}$Pu urine data from Los Alamos. A worker, not connected with identified incidents, received an intake over the regulatory limit of 50 mSv. Four post-intake urine samples were taken and all were analyzed using both RAS and TIMS. With TIMS data both after and before the intake, the situation is as well characterized as is practically possible over the limited time span of data collection. Calculations using only the first post-incident RAS data are compared with calculations using the entire dataset. It is found that the exact Poisson likelihood function needs to be used in order for the RAS result to agree with the final result. Using the Gaussian approximation, the first RAS data point does not alert one to what is coming.

The third case involves actual $^{238}$Pu urine data from Los Alamos. This is a realistic imperfect data set, and the proper interpretation is not readily apparent. Using prior information that the person had been involved in an incident, the MCMC calculation shows that only a single significant intake occurred, with a delayed-onset biokinetic response. Without using the incident prior information, several intakes in the same time period as the incident are calculated. Assuming a much large prior probability of intake (chronic intake situation), many intakes over the entire work history of the employee are calculated to be possible, however no individual intake is likely with any certainty. This seems to often be the case, that individual intakes, or even combined intakes in a year, may have occurred (we cannot rule them out), but we also cannot say with certainty that they have occurred.

The Markov Chain algorithm provides a definitive solution of the inverse problem of internal dosimetry, that of calculating the intake scenario given the bioassay data and an agreed-upon set of biokinetic models. By a definitive solution we mean an exact solution of the problem without simplifying assumptions.

The Bayesian method allows us to directly address the question of interest ("what is the dose?") and to quantify the uncertainties. The quantitative assessment of uncertainty is based on calculation of the probability distribution of intake parameters given the data. This is an inherently Bayesian quantity and such an analysis is not possible using non-Bayesian methods. Not surprisingly, it is simply not possible to identify the times of intakes with certainty in many cases, although other quantities, such as annual dose or total CEDE are usually relatively well determined by the data.

The drawback of this method is that it requires a large amount of computer time. Population studies involving thousands of cases, such as those carried out to determine the prior parameter $\alpha$(Miller et al. 2001) are not practical on a desktop workstation. Our future plans are to use massively parallel supercomputers to carry out such studies.

## References


Birchall, A., Jarvis, N. S., Pease, M. S., Riddell, A. E. & Battersby, W. P. (1998), 'The imba suite: Integrated modules for bioassay analysis', *Radiation Protection Dosimetry* pp. 107–110.

Gilks, W. R., Richardson, S. & Spiegelhalter, D. J. (1996), *Markov Chain Monte Carlo in Practice*, Chapman and Hall, New York.

Hickman, A. W., Griffith, W. C., Roessler, G. S. & Guilmette, R. A. (1995), 'Application of a Canine $^{238}$Pu Biokinetics/Dosimetry Model to Human Dosimetry Data', *Health Physics* **68**, 359–370.

Inkret, W. C., Efurd, D. W., Miller, G., Rokop, D. J. & Benjamin, T. M. (1998), 'Applications of Thermal Ionization Mass Spectrometry to the Detection of $^{239}$Pu and $^{240}$Pu Intakes', *International Journal of Mass Spectometry* **178**, 113–120.

Internation Commission on Radiological Protection (1988), *Recommendations of the International Commission on Radiological Protection, Individual Monitoring for Intakes of Radionuclides by Workers: Design and Interpretation*, Vol. 19 of *Annals of the ICRP*, Pergamon Press, Oxford. ICRP Publication 54.

International Commission on Radiological Protection (1979), *Limits for Intakes of Radionuclides by Workers*, Vol. 2 of *Annals of the ICRP*, Pergamon Press, New York. ICRP Publication 30, Part 1.

International Commission on Radiological Protection (1988), *Limits for Intakes of Radionuclides by Workers: an Addendum*, Vol. 19 of *Annals of the ICRP*, Pergamon Press, New York. ICRP Publication 30, Part 4.

International Commission on Radiological Protection (1994), *Human Respiratory Tract Model for Radiological Protection*, Vol. 24 of *Annals of the ICRP*, Pergamon Press, New York. ICRP Publication 66.

International Commission on Radiological Protection (1998), *Individual Monitoring for Internal Exposure of Workers, Replacement of ICRP Publication 54*, Vol. 27 of *Annals of the ICRP*, Pergamon Press, New York. ICRP Publication 78.

Lawrence, J. N. P. (1962), 'PUQFUA, An IBM 704 Code for Computing Plutonium Body Burdens', *Health Physics* **8**, 61.

Miller, G. (2000), *Applications of Probability and Statistics in Health Physics*, Medical Physics Publishing, chapter 9, pp. 323–330. (downloadable from www.lanl.gov/bayesian).

Miller, G. & Inkret, W. C. (1996), 'Bayesian Maximum Posterior Probability Method For Interpreting Plutonium Urinalysis Data', *Radiation Protection Dosimetry* **63**, 189–196.

Miller, G., Inkret, W. C., Little, T. T., Martz, H. F. & Schillaci, M. E. (2001), 'Bayesian Prior Probability Distributions for Internal Dosimetry', *Radiation Protection Dosimetry* **94**, 347–352.

Miller, G., Inkret, W. C. & Martz, H. F. (1999), 'Internal Dosimetry Intake Estimation Using Bayesian Methods', Radiation Protection Dosimetry 82, 5–17.

Miller, G., Inkret, W. C., Schillaci, M. E., Martz, H. F. & Little, T. T. (2000), 'Analyzing Bioassay Data Using Bayesian Methods–A Primer', Health Physics 78(6), 598–613.

Miller, G., Martz, H. F., Little, T. T. & Guilmette, R. (2002a), 'Bayesian Internal Dosimetry Calculations Using Markov Chain Monte Carlo', Radiation Protection Dosimetry 98(2), 191–198.

Miller, G., Martz, H. F., Little, T. T. & Guilmette, R. (2002b), 'Using Exact Poisson Likelihood Functions in Bayesian Interpretation of Counting Measurements', Health Physics . (to appear, LA-UR-01-2443).

Skilling, J., ed. (1989), Maximum Entropy and Bayesian Methods, Kluwer Academic Publishers, Dordrecht, The Netherlands.

Ward, R. C. & Eckerman, K. F. (1992), DOSEXPRT–A Bioassay Dosimetry Code for Martin Marietta Energy Systems, Inc., Technical Report ORNL/TM-11857, Oak Ridge National Laboratory.